

# Near-ideal lateral scaling in abrupt $\text{Al}_{0.48}\text{In}_{0.52}\text{As}/\text{In}_{0.53}\text{Ga}_{0.47}\text{As}$ heterostructure bipolar transistors prepared by molecular beam epitaxy

B. Jalali, R. N. Nottenburg, Y. K. Chen, A. F. J. Levi, D. Sivco, A. Y. Cho, and D. A. Humphrey

*AT&T Bell Laboratories, Murray Hill, New Jersey 07974*

(Received 22 February 1989; accepted for publication 25 March 1989)

We demonstrate near-ideal lateral scaling in abrupt junction  $\text{Al}_{0.48}\text{In}_{0.52}\text{As}/\text{In}_{0.53}\text{Ga}_{0.47}\text{As}$  heterostructure bipolar transistors. Current gain  $\beta = 162$  and  $122$  has been realized in transistors with emitter stripe width of  $50$  and  $0.6 \mu\text{m}$ , respectively. The excellent lateral scaling occurs because the  $0.5 \text{ eV}$  emitter injection energy results in nonequilibrium vertical electron transport in the thin ( $700 \text{ \AA}$ )  $\text{InGaAs}$  base.

Superior transport properties in  $\text{InGaAs}$  and compatibility with long-wavelength  $1.3\text{--}1.55 \mu\text{m}$  photonic devices suggest that  $\text{InGaAsP}$  heterostructure bipolar transistors (HBTs) should outperform  $\text{AlGaAs}$  HBTs in high-speed digital, optoelectronic, and microwave applications.<sup>1-10</sup> However, a useful low-power HBT requires small lateral dimensions while maintaining high current gain.

In this letter we show that near-ideal lateral scaling of transistors may be achieved by using nonequilibrium vertical electron transport through the device. Figure 1 shows the energy-band diagram of the  $\text{AlInAs}/\text{InGaAs}$  HBT used in this study. The abrupt emitter-base junction injects electrons into the base with energies that are considerably higher than the ambient thermal energy. Because of the high electron injection energy ( $0.5 \text{ eV}$ ) at the  $\text{AlInAs}/\text{InGaAs}$  emitter-base junction and conservation of electron wave vector parallel to the heterointerface, electrons are launched in a small angular cone perpendicular to the junction. Since extrinsic base recombination depends on the lateral transport of carriers, a high perpendicular to parallel electron velocity ratio ( $v_{\perp}/v_{\parallel}$ ) throughout the base results in better scaling. In bipolar transistors where carriers are injected with the ambient thermal energy ( $k_B T = 0.025 \text{ eV}$ )  $v_{\perp}/v_{\parallel}$  is small so that a small recombination velocity in the extrinsic base becomes a prerequisite for good lateral scaling. Therefore, an abrupt emitter with large injection energy and hence large  $v_{\perp}/v_{\parallel}$ , may be used to improve lateral scaling in a HBT.

Because of the heavier effective mass in the satellite valleys and the momentum relaxation association with intervalley scattering,<sup>11</sup> a large valley separation in the base is desirable. The  $\Gamma$ - $L$  energy separation in  $\text{InGaAs}$  is  $0.55 \text{ eV}$  compared to  $0.33 \text{ eV}$  in  $\text{GaAs}$ . Thus electrons may be injected with much higher energies without suffering intervalley scattering. We demonstrate for the first time that excellent lateral device scaling may be achieved using an abrupt  $\text{AlInAs}$  "launcher" with a  $0.5 \text{ eV}$  injection energy.

The layer structure described in Table I was grown by molecular beam epitaxy (MBE) on a semi-insulating  $\langle 100 \rangle$   $\text{InP}$  substrate. The substrate was polished with bromine methanol and then etched in  $\text{H}_2\text{SO}_4:\text{H}_2\text{O}_2:\text{H}_2\text{O}$  (4:1:1) solution for 10 min followed by a 3 min etch in 0.3% bromine methanol.<sup>12</sup> The surface oxide was desorbed in the MBE system at a temperature of  $530 \text{ }^\circ\text{C}$  while an  $\text{As}_4$  beam was used to stabilize the surface. High-purity solid sources of As,

Al, Ga, In, Si, and Be were used in the effusion cells, and the substrate was maintained at  $540 \text{ }^\circ\text{C}$  with a growth rate of  $2 \mu\text{m/h}$  for the entire growth sequence. The base was doped to  $p = 2 \times 10^{19} \text{ cm}^{-3}$  with Be. Transistors with emitter stripe size of  $0.6 \times 7$ ,  $1.1 \times 7$ ,  $1.6 \times 7$ ,  $2.6 \times 7$ ,  $3.6 \times 14$ , and  $50 \times 50 \mu\text{m}^2$  were fabricated.

Figure 2 shows the common-emitter characteristics of a typical HBT with emitter dimension  $3.6 \times 14 \mu\text{m}^2$ . At a collector current  $I_C = 1 \text{ mA}$  a current gain  $\beta = 150$  is measured. The measured offset voltage in the common-emitter characteristics is in agreement with an  $\text{AlInAs}/\text{InGaAs}$  conduction-band offset of  $\Delta E_c = 0.5 \text{ eV}$ .<sup>13</sup> Because of the large injection energy  $\Delta E_c$  and the thin base, electrons arrive at the collector depletion region with excess energy and can initiate avalanche multiplication even at small base-collector bias. This causes the nonsaturating collector current observed in Fig. 2. In an optimized device structure the collector thickness must be kept small in order to reduce the multiplication volume. The use of a wider band-gap collector will also improve the breakdown voltage. The negative differential resistance (hump) in the output characteristics is due to the device heating.

Figure 3 shows the transfer characteristics of the collector current  $I_C$  and the base current  $I_B$  as a function of the base-emitter voltage  $V_{BE}$  for the device with  $0.6 \times 7 \mu\text{m}^2$  emitter dimensions. The measured ideality factors are 1.3 and 1.5 for the collector current and base current, respectively. The ideality factor for the collector current depends only on the injection mechanism of electrons into the base. Therefore, we speculate that the nonideal part of the collector cur-

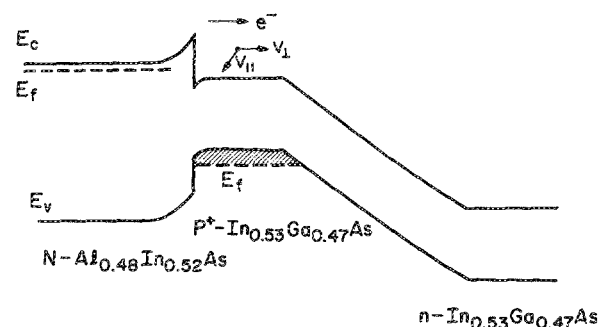


FIG. 1. Energy-band diagram for the  $\text{AlInAs}/\text{InGaAs}$  heterostructure bipolar transistor.

TABLE I. HBT layer structure.

Device layer	Doping (cm <sup>-3</sup> )	Thickness (Å)
n-InGaAs	1 × 10 <sup>19</sup>	2000
N-AlInAs	1 × 10 <sup>19</sup>	1000
N-AlInAs	5 × 10 <sup>17</sup>	2000
u-InGaAs	...	100
p-InGaAs	2 × 10 <sup>19</sup>	700
n-InGaAs	5 × 10 <sup>15</sup>	3000
n-InGaAs	1 × 10 <sup>19</sup>	5000
S.I.	InP	...

rent is due to tunneling of electrons at the emitter-base junction. This is not unlikely given the large  $\Delta E_c$  between AlInAs and InGaAs. The ideality factor for the base current was independent of emitter size indicating negligible perimeter effects. Because of nonequilibrium electron transport and the narrow base width, negligible recombination occurs in the intrinsic and extrinsic base layer.

Figure 4 shows the current gain  $\beta$  as a function of collector current for transistors with different emitter dimensions. The maximum current gain for the  $0.6 \times 7 \mu\text{m}^2$  device was 122 at an emitter current density of  $2.4 \times 10^4 \text{ A/cm}^2$ . The interesting feature is the high current gain at low density and the small change in  $\beta$  with different emitter dimensions. These results are dramatically better than those for AlGaAs/GaAs<sup>14</sup> and represent an improvement over those for the InP/InGaAs heterostructure.<sup>8</sup> This near-ideal lateral scaling may be attributed to the higher injection energy and therefore larger  $v_{\perp}/v_{\parallel}$  ratio in the base of the device with the AlInAs emitter compared to the InP emitter. It should be noted that the peak velocity of electrons in the InGaAs base is approximately constant (around  $1 \times 10^8 \text{ cm s}^{-1}$ ) in the energy range from 0.3 to 0.5 eV. However, the 0.5 eV injection energy in our devices results in an electron velocity which is insensitive to small decreases in energy ( $\sim 100 \text{ meV}$ ) resulting from inelastic scattering events. In this case a much higher average velocity may be maintained inside the

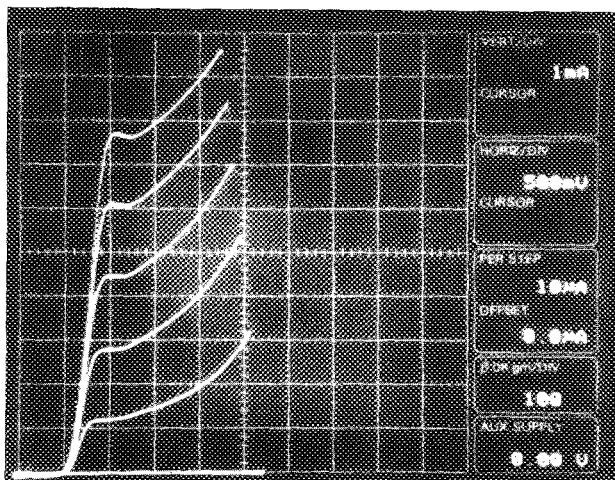


FIG. 2. AlInAs/InGaAs HBT common-emitter characteristics ( $I_C - V_{CE}$ ) for a transistor with emitter size  $3.6 \times 14 \mu\text{m}^2$ .

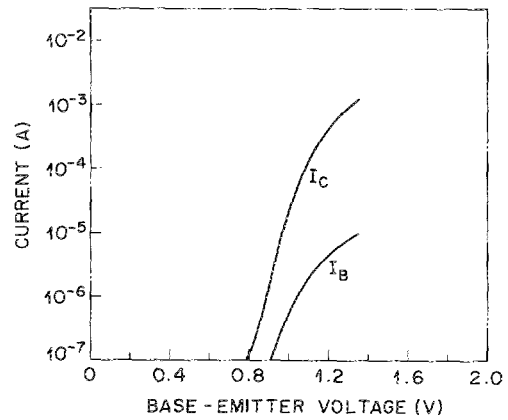


FIG. 3. Transfer characteristics of the collector current  $I_C$  and base current  $I_B$  as a function of the base-emitter voltage for transistor with emitter size of  $0.6 \times 7 \mu\text{m}^2$ .

base. Therefore, the base thickness or its doping may be increased without a significant reduction of the electron velocity. This fact permits greater flexibility in trade-off between base resistance (base doping level) and base transit time (base thickness).

The current gain roll-off in Fig. 4 occurs at a relatively low emitter current density ( $\sim 10^4 \text{ A/cm}^2$ ). However, previous work on InP/InGaAs HBTs has shown that current densities of  $10^5 \text{ A/cm}^2$  are achievable.<sup>10</sup> The maximum current density in our transistors is limited by electron supply in the relatively low-doped N-type emitter. Nevertheless, preliminary high-frequency measurements on our devices give a unity current gain cutoff frequency  $f_T$  of 60 GHz.

In summary, we have observed enhanced scaling in an AlInAs/InGaAs HBT. This behavior is attributed to high average electron velocity in the base caused by the large injection energy  $\Delta E_c$  of the abrupt AlInAs/InGaAs junction. The AlInAs emitter takes advantage of the large  $\Gamma$ -L valley separation in the InGaAs base by injecting electrons just below this separation. In this way extreme nonequilibrium electron transport in the base introduces a new flexibility in transistor design which, with proper exploitation, will result in ultrahigh-speed devices.

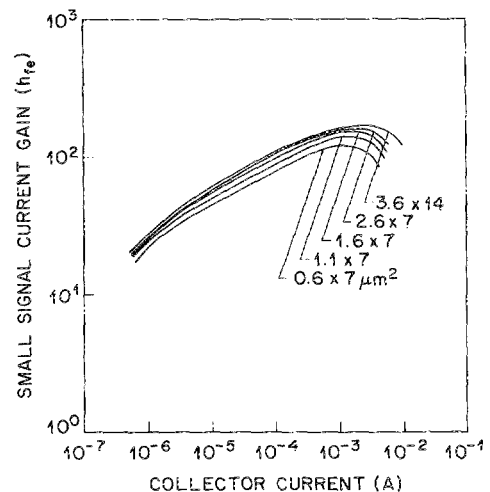


FIG. 4. Common-emitter gain as a function of collector current for different emitter dimensions  $0.6 \times 7$ ,  $1.1 \times 7$ ,  $1.6 \times 7$ ,  $2.6 \times 7$ ,  $3.6 \times 14 \mu\text{m}^2$ .

- <sup>1</sup>D. Fritzsche, E. Kuphal, and R. Aulbach, *Electron. Lett.* **17**, 178 (1981).
- <sup>2</sup>H. Kanbe, J. C. Vitek, and C. G. Fonstad, *IEEE Electron Device Lett.* **EDL-5**, 172 (1984).
- <sup>3</sup>R. N. Nottenburg, H. Temkin, M. B. Panish, R. Bhat, and J.-C. Bischoff, *IEEE Electron Device Lett.* **EDL-7**, 8 (1986).
- <sup>4</sup>O. Sugiura, A. G. Dentai, C. H. Joyner, S. Chandrasekhar, and J. C. Campbell, *IEEE Electron Device Lett.* **EDL-9**, 253 (1988).
- <sup>5</sup>R. J. Malik, J. R. Hayes, F. Capasso, K. Alavi, and A. Y. Cho, *IEEE Electron Device Lett.* **EDL-4**, 383 (1983).
- <sup>6</sup>W. Lee and C. G. Fonstad, *IEEE Electron Device Lett.* **EDL-7**, 683 (1986).
- <sup>7</sup>T. Won, C. K. Peng, J. Chyi, and Hadis Morkoc, *IEEE Electron Device Lett.* **EDL-9**, 334 (1988).
- <sup>8</sup>R. N. Nottenburg, Y. K. Chen, M. B. Panish, R. Hamm, and D. A. Humphrey, *IEEE Electron Device Lett.* **EDL-9**, 524 (1988).
- <sup>9</sup>H. Fukano, Y. Kawamura, and Y. Takanashi, *IEEE Electron Device Lett.* **EDL-9**, 312 (1988).
- <sup>10</sup>R. N. Nottenburg, Y. K. Chen, M. B. Panish, D. A. Humphrey, and R. Hamm, *IEEE Electron Device Lett.* **EDL-10**, 30 (1989).
- <sup>11</sup>M. Kuzuhara, K. Kim, and K. Hess, *IEEE Trans. Electron Devices* **ED-36**, 118 (1989).
- <sup>12</sup>A. Y. Cho, *Thin Solid Films* **100**, 291 (1983).
- <sup>13</sup>R. People, K. W. Wecht, K. Alavi, and A. Y. Cho, *Appl. Phys. Lett.* **43**, 118 (1983).
- <sup>14</sup>O. Nakajima, K. Nagata, H. Ito, T. Ishibashi, and T. Sugeta, *Jpn. J. Appl. Phys.* **24**, L596 (1985).